Journal of Nuclear Medicine, published on November 17, 2022 as doi:10.2967/jnumed.122.264434

Title: The association of age-related and off-target retention with longitudinal quantification of [^{18}F]MK6240 tau-PET in target regions.

Cécile Tissot BSc[1,2,3], Stijn Servaes PhD[1,2], Firoza Z. Lussier MSc[3], João Pedro Ferrari-Souza[3,4], Joseph Therriault BSc[1,2], Pâmela C. L. Ferreira PhD[3], Gleb Bezgin PhD[1,2], Bruna Bellaver PhD[3,4], Douglas Teixeira Leffa MD PhD[3], Sulantha S. Mathotaarachchi MSc[1,2], Mira Chamoun PhD[1,2], Jenna Stevenson BA[1,2], Nesrine Rahmouni BSc[1,2], Min Su Kang PhD[5,6], Vanessa Pallen BA[1,2], Nina Margherita-Poltronetti MSc[1,2], Yi-Ting Wang MSc[1,2], Jaime Fernandez-Arias MSc[1,2], Andrea L. Benedet PhD[7], Eduardo R. Zimmer PhD[4,8], Jean-Paul Soucy MD MSc[9], Dana L. Tudorascu PhD[3], Annie D. Cohen PhD[3], Madeleine Sharp MD[9], Serge Gauthier MD[2,10], Gassan Massarweh PhD[11], Brian Lopresti MSc[12], William E. Klunk PhD[3], Suzanne L. Baker PhD[13], Victor L. Villemagne MD[3], Pedro Rosa-Neto MD PhD[1,2,9,10], Tharick A. Pascoal MD PhD[3].

[1]McGill University, Montreal, Canada
[2]McGill University Research Center for Studies in Aging, Montreal Canada
[3]Departments of Psychiatry and Neurology, University of Pittsburgh School of Medicine, Pittsburgh, USA
[4]Graduate Program in Biological Sciences: Biochemistry, Porto Alegre, Brazil
[5]Artificial Intelligence and Computational Neurosciences lab, Sunnybrook Research Institute, University of Toronto, Toronto, Canada
[6]LC Campbell Cognitive Neurology Unit, Hurvitz Brain Sciences Program, Sunnybrook Research Institute, University of Toronto, Toronto, Canada
[7]University of Gothenburg, Gothenburg, Sweden
[8]Department of Pharmacology, Universidade Federal do Rio Grande do Sul, Porto Alegre, Brazil
[9]Montreal Neurological Institute, Montreal, Canada
[10]Douglas Mental Health Institute, Verdun, Canada
[11]Department of Radiochemistry, Montreal Neurological Institute, Montreal, Canada
[12]Department of Radiology, University of Pittsburgh School of Medicine, Pittsburgh, USA
[13]Department Lawrence Berkeley National Laboratory, Berkeley, United States of America

Corresponding author:
Tharick Pascoal, MD PhD
Assistant Professor of Psychiatry and Neurology
University of Pittsburgh
3501 Forbes Ave, Pittsburgh, PA 15213 – USA
Phone number: +1 412 246 5147
pascoalt@upmc.edu

First author:
Cécile Tissot, BSc, PhD candidate
McGill University
6825 Boulevard LaSalle Montreal, QC H4H 1R3 – Canada
Phone number : +1 514 766 2010
cecile.tissot@mail.mcgill.ca

Running title: [^{18}F]MK6240 age and off-target retention

Financial support: This work has been supported by the Weston Brain Institute, Fonds de Recherche Santé Québec, Healthy Brain for Healthy Lives and McGill University Faculty of Medicine. T.A.P. is supported by the Alzheimer's Association (no. AACSF-20-648075) and the National Institute of Health (NIH) (nos. R01AG073267 and R01AG075336).

Abstract:

[^{18}F]MK6240 tau-PET tracer quantifies brain tau neurofibrillary tangles (NFT) load in Alzheimer's disease (AD). The aims of our study are to test the stability of common reference region estimates in the cerebellum over time and across diagnoses and evaluate the effects of age-related and off-target retention on the longitudinal quantification of [^{18}F]MK6240 in target regions.

Methods: We assessed reference, target, age-related and off-target regions in 125 individuals across the aging and AD spectrum with longitudinal [^{18}F]MK6240 standardized uptake values (SUV) and ratios (SUVR) (2.25±0.40 years of follow-up duration). We obtained SUVR from meninges, exhibiting frequent off-target retention with [^{18}F]MK6240. Additionally, we compared tracer uptake between 37 cognitively unimpaired (CU) young (CUY, mean age: 23.41±3.33 years) and 27 CU older adults (CU, amyloid-β and tau negative, mean age: 58.50±9.01 years) to identify possible, non-visually apparent, age-related signal. Two-tailed t-test and Pearson correlations tested the difference between groups and associations between changes in region uptake, respectively.

Results: Inferior cerebellar grey (CG) SUV did not differ based on diagnosis and Aβ status, cross-sectionally and over time. [^{18}F]MK6240 uptake was significantly different between CUY and CU older adults in putamen/pallidum (affecting ~75% of the region) and in Braak II region (affecting ~35%). Changes in meningeal and putamen/pallidum SUVRs were not significantly different from zero, nor varied across diagnostic groups. We did not observe significant correlations between longitudinal changes in age-related or meningeal off-target retention and changes in target regions, whereas changes in all target regions were highly correlated.

Conclusion: Inferior CG was similar across diagnostic groups cross-sectionally and stable over time, thus deemed a suitable reference region for quantification. Despite not being visually perceptible, [^{18}F]MK6240 has age-related retention in subcortical regions, in much lower magnitude but topographically co-localized with significant off-target signal of the first-generation tau tracers. The lack of correlation between changes in age-related/meningeal and target retention suggests little influence of possible off-target signals on longitudinal tracer quantification. Nevertheless, the age-related retention in Braak II needs to be further investigated. Future post-mortem studies should elucidate the source of the newly reported age-related [^{18}F]MK6240 signal, and *in vivo* studies further explore its impact on tracer quantification.

Key words: tau, positron emission tomography, reference region, off-target binding, [^{18}F]MK6240.

Introduction:

Accumulation of amyloid-β (Aβ) plaques and hyperphosphorylated tau, forming neurofibrillary tangles (NFT), are hallmarks of Alzheimer's disease (AD)(*1*) and can be observed in aging and AD dementia(*2*). Assessment of the tau levels in the brain is done through cerebrospinal fluid and positron emission tomography (PET) imaging. Radiotracers used in PET imaging are considered optimal when they present desirable characteristics such as rapidly equilibrating *in vivo* kinetics, low off-target retention, no significant lipophilic radiolabeled metabolites able to enter the brain and high affinity for their target(*3*).

[^{18}F]MK6240 is a promising tracer allowing for the quantification of fibrillar tau pathology *in vivo* with post-mortem studies confirming its binding to paired helical fragments of phosphorylated tau(*4*–*7*). The tracer binds with high affinity to NFT, thus making it specific for AD-related tauopathy. As shown in post-mortem data, the tracer does not seem to bind to tau aggregates in non-AD tauopathies(*5*,*8*), except in rare frontotemporal dementia mutations associated with brain deposition of NFT(*9*). [^{18}F]MK6240 allows for the differentiation between cognitively unimpaired (CU), mild cognitive impairment (MCI), and AD subjects(*4*). Furthermore, [^{18}F]MK6240 has been shown to recapitulate *in vivo* the tau pathologic stages, proposed via post-mortem studies by Braak and colleagues(*10*,*11*).

Despite several favorable features of [^{18}F]MK6240, some common challenges in PET studies remain unaddressed for this tracer, such as the choice of a reference region for longitudinal studies and the impact of off-target retention on tracer quantification in target regions (i.e. regions expected to show specific, tau-related retention of [^{18}F]MK6240). Post-mortem and *in vivo* studies

have indicated that [^{18}F]MK6240 has off-target retention in neuromelanin-containing cells(*5*). Those are regions also observed using first-generation tau-PET tracers such as the substantia nigra (*12*). However, [^{18}F]MK6240 shows significant off-target retention in the meninges(*4*,*13*), which is currently the main concern for accurate quantification of NFT using this tracer.

As longitudinal tracer quantification is critical for clinical trials using tau-PET imaging agents as a possible surrogate marker of tau accumulation, exploring the optimal reference region and the effects of off-target retention on longitudinal [^{18}F]MK6240 quantification is crucial(*14*,*15*). Here, we studied longitudinal changes in reference, target, age-related, and off-target regions across diagnostic groups and Aβ status to elucidate the caveats associated with the longitudinal quantification of [^{18}F]MK6240.

Materials and Methods:

Participants

We included individuals from the TRIAD cohort(*16*), with data obtained from December 2017 to November 2021. The study was approved by the Douglas Mental Institute Research Board and all participants gave written consent. Detailed information gathered from the participants can be found here: https://triad.tnl-mcgill.com/. All participants underwent a complete neuropsychological evaluation, magnetic resonance imaging (MRI), and acquisition of both [^{18}F]AZD4694 (Aβ) and [^{18}F]MK6240 (tau) PET scans. We used two distinct subject samples for the analyses described in this work. To assess age-related off-target retention of [^{18}F]MK6240, we included 37 cognitively unimpaired young (CUY <35 years of age) and 27 cognitively unimpaired older adults (CU 40-65 years of age), both presenting no AD-related pathology (Aβ and tau); this sample was called "age-

related sample" and only included cross-sectional data. Aβ status was determined as [^{18}F]AZD4694 global PET SUVR lower than 1.55 SUVR(*17*), while tau status was determined with [^{18}F]MK6240 temporal meta-ROI lower than 1.24 SUVR, as previously described (*18*). The longitudinal sample was composed of 125 individuals [11 CUY, 66 CU Aβ negative (Aβ-), 17 CU Aβ positive (Aβ+), and 31 cognitively impaired (CI) Aβ+, including 22 multi-domain amnestic MCI and 9 AD] who underwent a follow-up assessment between 1.5 and 3.5 years after their baseline. Baseline diagnosis was used in the analyses, following clinical assessments as well as Mini-Mental State Examination (MMSE), and Clinical Dementia Rating (CDR) scores and the NIA-AA criteria(*19*). CU individuals did not have an objective impairment, MMSE score of 26 or more and CDR score of 0(*20*). Individuals diagnosed with mild cognitive impairment (MCI) had subjective and/or objective cognitive impairment, relatively preserved activities of daily life, as assessed with an MMSE score of 26 or above and CDR of 0.5(*21*). Dementia due to AD was assessed with an MMSE score of less than 26 and a CDR score of 0.5 or more. No participant met the criteria for another neurological or major neuropsychiatric disorder following a clinical interview performed by a trained physician.

PET image processing:

Participants underwent a T1-weighted MRI (3T, Siemens), as well as [^{18}F]MK6240 tau-PET and [^{18}F]AZD4694 Aβ-PET using the same brain-dedicated Siemens high resolution research tomograph. [^{18}F]MK6240 images were acquired 90-110 minutes post tracer injection and reconstructed using an ordered subset expectation maximization (OSEM) algorithm on a 4D volume with four frames (4 x 300 s)(*4*). [^{18}F]AZD4694 images were acquired 40-70 minutes post tracer injection, and reconstructed with the same OSEM algorithm with three frames (3 x 600s)(*4*).

Each PET acquisition was finished with a 6-min transmission scan with a rotation ^{137}Cs point source for attenuation correction. Images were further corrected for motion, decay, dead time, and random and scattered coincidences. Standardized uptake value (SUV) images were calculated considering the injected radionuclide dose and weight of each participant ($\frac{PET}{dose/weight}$). Injected dose and weight information can be found in the supplementary material (Supplementary Table 1). SUV values were extracted from the inferior cerebellar grey (CG), superior CG, Crus I, and full CG. Information on the masks can be found in Supplementary Table 2. SUV ratio (SUVR) images were generated using the inferior CG as the reference region for [^{18}F]MK6240 and full CG for [^{18}F]AZD4694. Finally, images were spatially smoothed to achieve a final Gaussian kernel of full width half maximum (FWHM) of 8 mm(*22*,*23*). Supplementary Table 3 outlines the mean sensitivity of the scanner at baseline and follow-up visits. Meninges were not masked at any step of the processing for the present study. A populational-based meningeal mask was created with the Montreal Neurological Institute (MNI) MINC-toolkit as the region having >90% of probability of being part of either telencephalon or cerebellar meninges in CUY individuals (Supplementary Figure 1). In addition, we divided individuals as having high and low meningeal retention, based on the meninges' SUV median of the population. SUVR values in Braak regions were extracted following Pascoal *et al*(*10*). Additionally, the Desikan-Killiany-Tourville (DKT) atlas(*24*) was used to obtain [^{18}F]MK6240 SUVR from the putamen and the pallidum. A global [^{18}F]AZD4694 SUVR value was estimated by averaging the SUVR from the precuneus, prefrontal, orbitofrontal, parietal, temporal, anterior, and posterior cingulate cortices(*25*). The cut-off value for Aβ positivity used is a published threshold of 1.55(*17*) global SUVR, applied to classify participants as Aβ positive (Aβ+) or Aβ negative (Aβ-). MNI MINC-toolkit was used to calculate average images of [^{18}F]MK6240 retention.

Statistical analyses:

R statistical software (version 4.0.0) was used to perform non-imaging statistical analyses. T-tests or ANOVA tests were conducted for continuous variables and chi-square or Fisher tests for categorical variables for demographic information when appropriate. The coefficient of variation (COV) was calculated as the group standard deviation divided by the mean. Longitudinal change (Δ) was calculated as follows: $\frac{(follow\text{-}up\ SUV(R)\ -baseline\ SUV(R))}{time\ (years)}$. Associations between changes in biomarkers were assessed with Pearson correlation. Voxel-wise statistical comparisons were conducted using VoxelStats, a statistical toolbox implemented in MATLAB(*26*). The age-related retention was evaluated at the voxel level conducting a two-sided t-test, between CUY and CU Aβ and tau negative elderly individuals aged from 40 to 65 years (Table 1.A). False discovery rate correction was applied with a voxel-level correction of $p < 0.05$.

Results:

Participants:

In the age-related group analyses, comparing CUY and CU older adults who were both Aβ and tau negative, we observed no significant difference in sex and years of education. By definition, subjects had a significant difference in age. We also observed a small but significant difference in the MMSE score, with the CU older adults having a slightly lower score (Table 1). In the longitudinal dataset, as expected, we observed significant differences in the age, MMSE and CDR scores across groups. There was no difference in the years of education; however, a small but significant difference was observed regarding sex with more females in the CUY and CU Aβ+ groups (Table 2).

Assessment of stability of reference regions over time for use in longitudinal studies

Our first objective was to ascertain the reference region appropriateness for longitudinal quantification of [^{18}F]MK6240. Using the change of SUV over time (ΔSUV), we tested the stability of SUV over the time frame of our study in the inferior CG, superior CG, cerebellar Crus I, and full CG. No significant differences in the longitudinal changes were observed when separating individuals based on their clinical diagnosis (Figure 1.A), Aβ status (Figure 1.B), or both (Figure 1.C). Mean and standard deviation of ΔSUV can be found in Supplementary Table 4. Coefficients of variation of [^{18}F]MK6240 ΔSUV were similar with the highest numerical value in the inferior CG longitudinal change (-12.64), whereas the Crus I presented the lowest (-3.71) (Figure 1.D, Table 3). We observed no significant variability in SUV value (i.e. between baseline and follow-up measures) in the assessed reference regions (Table 4, Supplementary Table 5).

Supplementary material displays the cross-sectional differences in those SUV values. In the cross-sectional analysis, only superior CG (CU-AD *p*-value <0.001, MCI-AD *p*-value <0.001) and Crus I (CU-AD *p*-value = 0.046, MCI-AD *p*-value = 0.051) presented significant differences between diagnostic groups after correction for multiple comparisons (Supplementary Figure 2). Cross-sectional coefficients of variation of reference regions are reported in Supplementary Figure 3.

Meningeal and age-related retentions:

Figure 2.A represents the average [^{18}F]MK6240 SUVR values in the CUY group. First, we detected a strong correlation between telencephalon and cerebellar meninges, cross-sectionally and longitudinally (Supplementary Figure 4). We observed no significant difference between

diagnostic groups in the telencephalon meninges cross-sectionally [CU Aβ- vs CU Aβ+ *p*-value = 0.891; CU Aβ- vs CI Aβ+ *p*-value = 0.797; CU Aβ+ vs CI Aβ+ *p*-value = 0.999] and longitudinally [CU Aβ- vs CU Aβ+ *p*-value = 0.150; CU Aβ- vs CI Aβ+ *p*-value = 0.677; CU Aβ+ vs CI Aβ+ *p*-value = 0.524]. Similarly, no differences were observed in the cerebellar meninges neither cross-sectionally [CU Aβ- vs CU Aβ+ *p*-value = 0.946; CU Aβ- vs CI Aβ+ *p*-value = 0.919; CU Aβ+ vs CI Aβ+ *p*-value = 0.837] nor in longitudinal changes [CU Aβ- vs CU Aβ+ *p*-value = 0.563; CU Aβ- vs CI Aβ+ *p*-value = 0.631; CU Aβ+ vs CI Aβ+ *p*-value = 0.963] (Figure 2.B). Finally, females showed higher SUVR values in the meninges compared to males transversally, but not longitudinally (Supplementary Figure 5).

Average [^{18}F]MK6240 SUVR images of CUY and CU Aβ and tau negative individuals, less than 65 years of age, did not seem to display striking visual differences. However, a t-test between the two groups revealed significantly higher [^{18}F]MK6240 retention in the putamen, the pallidum, a parcel of cerebellar white matter, as well as a few other cortical regions (Figure 3.A). The same test was carried out in the longitudinal sample as well (Supplementary Figure 6). We assessed the percentage of overlap between the age-related signal and brain regions. The most important regional overlaps were observed with the putamen (75% of the region showing overlap), pallidum (72%), followed by Braak stage II region (38%) (Figure 3.B). SUVR values in the putamen and pallidum were significantly different among diagnostic groups, with the CUY having a significantly lower [^{18}F]MK6240 retention cross-sectionally [CUY vs CU Aβ- *p*-value < 0.001; CUY vs CU Aβ+ *p*-value < 0.001; CUY vs CI Aβ+ *p*-value < 0.001]. Additionally, the CI Aβ+ individuals had significantly higher values as compared to CU (Aβ- and Aβ+) cross-sectionally [CU Aβ- vs CU Aβ+ *p*-value = 0.926; CU Aβ- vs CI Aβ+ *p*-value < 0.001; CU Aβ+ vs CI Aβ+ *p*-

value < 0.001]. Nevertheless, the longitudinal rate of change (ΔSUVR) did not present significant differences among the groups [CUY vs CU Aβ- *p*-value = 0.927; CUY vs CU Aβ+ *p*-value = 0.845; CUY vs CI Aβ+ *p*-value = 0.731; CU Aβ- vs CU Aβ+ *p*-value = 0.880; CU Aβ- vs CI Aβ+ *p*-value = 0.728; CU Aβ+ vs CI Aβ+ *p*-value = 0.994] (Figure 3.C).

Associations of changes in target, age-related, and off-target retention:

Target regions were considered brain regions in which we expect to see [^{18}F]MK6240 retention based on the pattern of tau distribution extensively reported in the post-mortem literature(*1*,*27*). We found a strong correlation between ΔSUVR in target regions with each other, where each Braak region was more strongly correlated with the adjacent stages. The weakest correlation was depicted between Braak I and Braak VI regions. When extracting the average SUVR in Braak I-III and Braak IV-VI, we also observed a strong positive correlation between regions (R = 0.62, *p*-value < 0.001). We then used SUVR values in the telencephalon and cerebellar meninges, as well as the putamen and pallidum in the correlations. ΔSUVR in those regions did not correlate significantly with ΔSUVR in any one of the target regions [Braak I-III and telencephalon meninges: R = -0.03, *p*-value = 0.740; Braak IV-VI and telencephalon meninges: R = 0.10, *p*-value = 0.290; Braak I-III and cerebellar meninges: R = -0.12, *p*-value = 0.200; Braak IV-VI and cerebellar meninges: R = -0.02, *p*-value = 0.870; Braak I-III and putamen & pallidum: R = 0.12, *p*-value = 0.200; Braak IV-VI and putamen & pallidum: R = 0.05, *p*-value = 0.600]. Nor did the meningeal and putamen/pallidum ΔSUVR correlate with each other [R = 0.01, *p*-value = 0.920] (Figure 4). To further assess the impact of meninges in tracer' quantification, we divided individuals in high and low meningeal retention groups (based meninges SUV median). We did not find difference of diagnostic groups or longitudinal tracer accumulation between individuals

with high and low meningeal retention (Supplementary Table 6). Finally, we assessed the stability of [^{18}F]MK6240 SUVR in target regions over time, when using different reference regions (i.e. inferior CG, Crus I, full CG and superior CG). We extracted Braak IV-VI SUVR values in CUY and CU Aβ- individuals, where we do not expect significant increase of SUVR values. We observed no difference between baseline and follow-up values when using either reference region (Supplementary Figure 7, Supplementary Table 7).

Discussion:

This study suggests that the most widely used cerebellar reference regions (inferior CG, superior CG, Crus I, and full CG) present stability, with no changes over time, and therefore may be suitable for use in longitudinal studies, although differences were observed in superior CG and Crus I cross-sectionally. We provide evidence for the existence of an age-related retention in the putamen/pallidum, similar, albeit of much lower magnitude, to the reported off-target retention observed using the first-generation tau-PET tracers(*12*,*28*). Finally, we demonstrated that there was no association between [^{18}F]MK6240 ΔSUVR in target regions and in age-related or meningeal off-target signals over the time frame of our study.

Previous cross-sectional studies have already shown that indices of tau load made using [^{18}F]MK6240 are amenable to simplified tissue ratio methods using data acquired 90-110 minutes post-injection(*4*,*7*). However, questions remain regarding the suitability of the reference region for longitudinal tracer quantification due to the bias often inherent to SUVR data(*10*). This is of paramount importance because [^{18}F]MK6240 has been used in clinical trial settings to capture longitudinal changes in tau tangle pathology(*29*). Extensive research has been conducted focusing

on the cerebellum as the appropriate reference region for tau radiotracers(*30*,*31*), as the CG is not expected to harbor significant NFT pathology (*1*). Although the gold standard method for the assessment of the optimal reference region relies on dynamic quantifications with arterial input function, one crucial characteristic of a reference region for longitudinal assessments is not having large variability over time, across diagnostic groups or other pathological features (i.e., Aβ status in the case of AD research)(*32*). In this study, we estimated the [^{18}F]MK6240 SUV values in distinct regions of the cerebellar grey matter at baseline, as well as its change over time, based on diagnosis and on Aβ status. Results indicate that there were small cross-sectional differences between diagnostic groups in the superior CG and Crus I but not in the inferior CG and full CG. These differences might be due to spillover effect from the target regions, as individuals with AD dementia inherently have a higher uptake of the tracer. Additionally, we did not observe differences in the cerebellar SUVs based on Aβ status. When examining the differences between baseline and follow-up assessments, we did not observe any significant difference in [^{18}F]MK6240 SUV for any cerebellar region. Even though all variability was relatively minor, we observed the lowest numerical variability in the SUV levels of the inferior CG cross-sectionally and in the Crus I longitudinally. Altogether, our results suggest that tracer retention in the tested reference regions was relatively stable over time and across diagnostic groups, suggesting that all these reference regions could potentially be used for longitudinal [^{18}F]MK6240 quantification. Given the cross-sectional differences in tracer uptake among diagnostic groups in superior CG and Crus I but not in the inferior CG, this latter region was deemed more appropriate for the cross-sectional and longitudinal [^{18}F]MK6240 quantification, and thus used for the remaining analyses. Future studies using the gold standard arterial input function should address other important characteristics of an optimal reference region.

The t-test comparing young individuals under age 35 and participants between 40 and 65 years of age allowed us to assess age-related retention of [^{18}F]MK6240. The regions presenting the higher age-related [^{18}F]MK6240 retention were the putamen and pallidum. Those are often considered off-target regions using other radiotracers for tau(*31–33*), but it seems to be of lower magnitude with [^{18}F]MK6240(*34*). As we included participants younger than 65 years that were CU Aβ and tau negative, we do not expect on-target [^{18}F]MK6240 retention in subcortical structures based on the post-mortem literature(*35*). Indeed, subcortical regions have been shown to harbor NFT accumulation only at late Braak pathological stages (*27*,*36*), which might explain why we observed a significant cross-sectional difference in putamen and pallidum SUVR between CI Aβ+ individuals as compared to CU (either Aβ- or Aβ+). Similar to first-generation tau-PET tracers(*5*), the retention observed with [^{18}F]MK6240 in the putamen and pallidum may be due to neuromelanin deposition. While the tracer retention observed in Braak II can represent an age-related signal, we cannot entirely exclude that there is some true concentration of NFT in this region, as modest tau accumulation in CU Aβ- individuals has already been reported in the hippocampus (*2*,*35*). Another possibility is that the marked off-target retention of first-generation tracers in the choroid plexus(*12*), which contaminates the Braak II region for these tracers, could be a minor age-related problem with [^{18}F]MK6240 as well. However, it is important to note some individuals could potentially have primary age-related tauopathy (PART)(*37*), who are subjects harboring NFT accumulation in early Braak stages, with little to no Aβ deposition. Finally, we assessed meningeal retention in both telencephalon and cerebellar regions, which has already been characterized as off-target by previous post-mortem studies(*5*). Importantly, we observed no significant difference in the magnitude of meningeal uptake across diagnosis and Aβ status and no change over time. Nevertheless, we observed sex differences in meningeal retention cross-

sectionally but not longitudinally, as previously reported with other tau-PET tracers in the meninges and skull(*13*). Taken together, those results suggest that besides the meningeal retention, [^{18}F]MK6240 presents a newly described age-related retention in subcortical brain regions, in which the cause(s) need to be elucidated by future *in vitro* studies across the aging spectrum.

We observed no association between annualized [^{18}F]MK6240 SUVR changes in target, age-related regions, and meninges. Braak regions were used to represent target areas for tau tangles, as extensively reported in post-mortem studies(*1*,*27*). ΔSUVR values in target brain regions correlated strongly with each other, suggesting that changes in tracer retention in these brain regions are influenced by the same brain process, likely NFT accumulation(*22*). On the other hand, we did not observe a significant correlation between ΔSUVR in meningeal off-target uptake and changes in Braak target regions. Additionally, age-related ΔSUVR in the putamen and pallidum did not correlate with that in target regions. Nor did off-target, meningeal and age-related subcortical ΔSUVR correlate with each other. This suggests that different processes set the paces of progression in target, off-target, and age-related regions and that the spillover from off-target regions would not heavily influence rates of progression in [^{18}F]MK6240 target regions.

This study has limitations. The lack of arterial sampling at baseline and follow-up limits the assessments of reference region and accurate tracer retention. We observed a very small decrease in SUV values in cerebellar regions over time, close to zero, that was not statistically significant. Additionally, all [^{18}F]MK6240 analyses were conducted using images acquired from 90 to 110 minutes post-injection. Even though this simplified quantitative approach has been validated(*4*), dynamically acquired PET data with arterial input function would be more appropriate to test the

hypotheses of our study. Although there is a possibility that the effect of meninges in reference regions could lead to changes in baseline and follow-up values and, consequently, in rates of change, the fact that meninges uptake did not change significantly over time or differ between groups defined using cognition or amyloid-β status suggest that it does not play a major role in the longitudinal results provided by this tracer. Moreover, we presently used a spatial smoothing of 8mm; a smaller smoothing would likely have less impact of the meninges on the adjacent brain regions. An additional limitation is the lack of partial volume correction which was not conducted in our study. Post-mortem data would validate our findings, as it would allow us to ensure the absence of NFT in the cerebellar regions, as well as in the age-related retention regions. Without post-mortem confirmation, we cannot exclude that age-related retention in CU older adults is caused by tau tangle pathology. Moreover, our sample was restricted to a follow-up time of 1.5 to 3.5 years; by using other follow-up durations, we might obtain different results. In the current project, we evaluated only a small subset of reference regions that are frequently reported in the literature; it is possible that other regions might present better results for [^{18}F]MK6240 longitudinal quantification. An additional limitation is that we did not provide any evidence about the mechanism through which age-related retention occurs. Arterial and post-mortem data are needed to understand our findings.

Conclusion:

Inferior CG is a suitable reference region for the cross-sectional and longitudinal quantification of [^{18}F]MK6240. [^{18}F]MK6240 exhibits off-target retention in the meninges and an age-related signal in the putamen/pallidum, also likely representing off-target retention, and Braak II region in which the source needs to be elucidated. The lack of an association between changes in SUVR within

age-related, off-target, and target regions suggests that longitudinal changes in [^{18}F]MK6240 are not heavily driven by changes in age-related or off-target signals. However, future post-mortem studies are needed to clarify these findings.

Acknowledgments:

We thank Cerveau Technologies for providing us with [^{18}F]MK6240.

Financial support:

This work has been supported by the Weston Brain Institute, Fonds de Recherche Santé Québec, Healthy Brain for Healthy Lives and McGill University Faculty of Medicine. T.A.P. is supported by the Alzheimer's Association (no. AACSF-20-648075) and the National Institute of Health (NIH) (nos. R01AG073267 and R01AG075336).

Conflict of interest: S.G. has served as a scientific advisor to Cerveau Therapeutics. No other potential conflicts of interest relevant to this article exist.

Key points:

Question: What is the effect of reference region and non-target tracer retention in the longitudinal quantification of [^{18}F]MK6240 in target regions?

Pertinent findings: Our longitudinal observational study showed that the inferior and full cerebellar greys are appropriate reference regions for cross-sectional and longitudinal quantifications of [^{18}F]MK6240. This tracer is already known to present off-target binding in the meninges, but we discovered a so-called age-related binding in the putamen/pallidum. However, the longitudinal changes in non-target tracer retention do not correlate with longitudinal changes in on-target regions.

Implications for patient care: [^{18}F]MK6240 can be used as a surrogate marker in clinical trials, as long as the appropriate reference region is used, and off-target and age-related retention are considered.

References:

1. Braak H, Braak E. Neuropathological stageing of Alzheimer-related changes. *Acta Neuropathol*. 1991;82:239-259.
2. Jagust W. Imaging the evolution and pathophysiology of Alzheimer disease. *Nat Rev Neurosci*. 2018;19:687-700.
3. Lewis JS, Windhorst AD, Zeglis BM. Radiopharmaceutical chemistry.; 2019.
4. Pascoal TA, Shin M, Kang MS, et al. In vivo quantification of neurofibrillary tangles with [18 F]MK-6240. *Alzheimer's Res Ther*. 2018;10:1-15.
5. Aguero C, Dhaynaut M, Normandin MD, et al. Autoradiography validation of novel tau PET tracer [F-18]-MK-6240 on human postmortem brain tissue. *Acta Neuropathol Commun*. 2019;7:37.
6. Hostetler ED, Walji AM, Zeng Z, et al. Preclinical characterization of 18F-MK-6240, a promising PET tracer for in vivo quantification of human neurofibrillary tangles. *J Nucl Med*. 2016;57:1599-1606.
7. Betthauser TJ, Cody KA, Zammit MD, et al. In vivo characterization and quantification of neurofibrillary tau PET radioligand 18 F-MK-6240 in humans from Alzheimer disease dementia to young controls. *J Nucl Med*. 2019;60:93-99.
8. Iqbal K, Del C. Alonso A, Chen S, et al. Tau pathology in Alzheimer disease and other tauopathies. *Biochim Biophys Acta - Mol Basis Dis*. 2005;1739:198-210.
9. Levy JP, Bezgin G, Savard M, et al. 18F-MK-6240 tau-PET in genetic frontotemporal dementia. *Brain*. 2021:1-26.
10. Pascoal TA, Therriault J, Benedet AL, et al. 18F-MK-6240 PET for early and late detection of neurofibrillary tangles. *Brain*. 2020;143:2818-2830.

11. Therriault J, Pascoal TA, Lussier FZ, et al. Biomarker modeling of Alzheimer's disease using PET-based Braak staging. *Nat Aging*. 2022:1-10.
12. Lee CM, Jacobs HIL, Marquié M, et al. 18F-Flortaucipir Binding in Choroid Plexus: Related to Race and Hippocampus Signal. *J Alzheimer's Dis*. 2018;62:1691-1702.
13. Smith R, Strandberg O, Leuzy A, et al. Sex differences in off-target binding using tau positron emission tomography. *NeuroImage Clin*. 2021;31:102708.
14. Baker SL, Harrison TM, Maass A, Joie R La, Jagust WJ. Effect of off-target binding on 18F-flortaucipir variability in healthy controls across the life span. *J Nucl Med*. 2019;60:1444-1451.
15. Chen K, Roontiva A, Thiyyagura P, et al. Improved power for characterizing longitudinal amyloid-βPET changes and evaluating amyloid-modifying treatments with a cerebral white matter reference region. *J Nucl Med*. 2015;56:560-566.
16. Therriault J, Benedet AL, Pascoal TA, et al. APOEε4 potentiates the relationship between amyloid-β and tau pathologies. *Mol Psychiatry*. 2020;26:5977–5988.
17. Therriault J, Benedet AL, Pascoal TA, et al. Determining Amyloid-Beta positivity using [18F]AZD4694 PET imaging. *J Nucl Med*. 2020;62:247-252.
18. Therriault J, Pascoal TA, Benedet AL, et al. Frequency of Biologically Defined Alzheimer Disease in Relation to Age, Sex, APOE ε4, and Cognitive Impairment. *Neurology*. 2021;96:e975-e985.
19. Jack CR, Bennett DA, Blennow K, et al. NIA-AA Research Framework: Toward a biological definition of Alzheimer's disease. *Alzheimer's Dement*. 2018;14:535-562.
20. Jack CR, Wiste HJ, Schwarz CG, et al. Longitudinal tau PET in ageing and Alzheimer's disease. *Brain*. 2018;141:1517-1528.

21. Petersen RC. Mild cognitive impairment as a diagnostic entity. *J Intern Med*. 2004;256:183-194.

22. Pascoal TA, Benedet AL, Tudorascu DL, et al. Longitudinal 18F-MK-6240 tau tangles accumulation follows Braak stages. *Brain*. 2021;144:3517-3528.

23. Joshi A, Koeppe RA, Fessler JA. Reducing between scanner differences in multi-center PET studies. *Neuroimage*. 2009;46:154-159.

24. Desikan RS, Ségonne F, Fischl B, et al. An automated labeling system for subdividing the human cerebral cortex on MRI scans into gyral based regions of interest. *Neuroimage*. 2006;31:968-980.

25. Jack CR, Wiste HJ, Weigand SD, et al. Defining imaging biomarker cut points for brain aging and Alzheimer's disease. *Alzheimer's Dement*. 2017;13:205-216.

26. Mathotaarachchi S, Wang S, Shin M, et al. VoxelStats: A MATLAB package for multi-modal voxel-wise brain image analysis. *Front Neuroinform*. 2016;10:1-12.

27. Braak H, Braak E. Staging of Alzheimer's disease-related neurofibrillary changes. *Neurobiol Aging*. 1995;16:271-284.

28. Leuzy A, Chiotis K, Lemoine L, et al. Tau PET imaging in neurodegenerative tauopathies—still a challenge. *Mol Psychiatry*. 2019;24:1112-1134.

29. Knopman DS, Jones DT, Greicius MD. Failure to demonstrate efficacy of aducanumab: An analysis of the EMERGE and ENGAGE trials as reported by Biogen, December 2019. *Alzheimer's Dement*. 2021;17:696-701.

30. Lemoine L, Saint-Aubert L, Marutle A, et al. Visualization of regional tau deposits using (3)H-THK5117 in Alzheimer brain tissue. *Acta Neuropathol Commun*. 2015;3:40.

31. Marquie M, Normandin MD, Vanderburg CR, et al. Validating novel tau PET tracer [^{18}F]-

AV-1451 (T807) on postmortem brain tissue HHS Public Access. *Ann Neurol*. 2015;78:787-800.

32. Lohith TG, Bennacef I, Vandenberghe R, et al. Brain imaging of Alzheimer dementia patients and elderly controls with 18 F-MK-6240, a PET tracer targeting neurofibrillary tangles. *J Nucl Med*. 2019;60:107-114.

33. Collier TL, Yokell DL, Livni E, et al. cGMP production of the radiopharmaceutical [18F]MK-6240 for PET imaging of human neurofibrillary tangles. *J Label Compd Radiopharm*. 2017;60:263-269.

34. Gogola A, Minhas DS, Villemagne VL, et al. Direct Comparison of the Tau PET Tracers 18F-Flortaucipir and 18F-MK-6240 in Human Subjects. *J Nucl Med*. 2022;63:108-116.

35. Braak H, Thal DR, Ghebremedhin E, Del Tredici K. Stages of the pathologic process in alzheimer disease: Age categories from 1 to 100 years. *J Neuropathol Exp Neurol*. 2011;70:960-969.

36. Braak H, Alafuzoff I, Arzberger T, Kretzschmar H, Tredici K. Staging of Alzheimer disease-associated neurofibrillary pathology using paraffin sections and immunocytochemistry. *Acta Neuropathol*. 2006;112:389-404.

37. Hickman RA, Flowers XE, Wisniewski T. Primary Age-Related Tauopathy (PART): Addressing the Spectrum of Neuronal Tauopathic Changes in the Aging Brain. *Curr Neurol Neurosci Rep*. 2020;20:1-18.

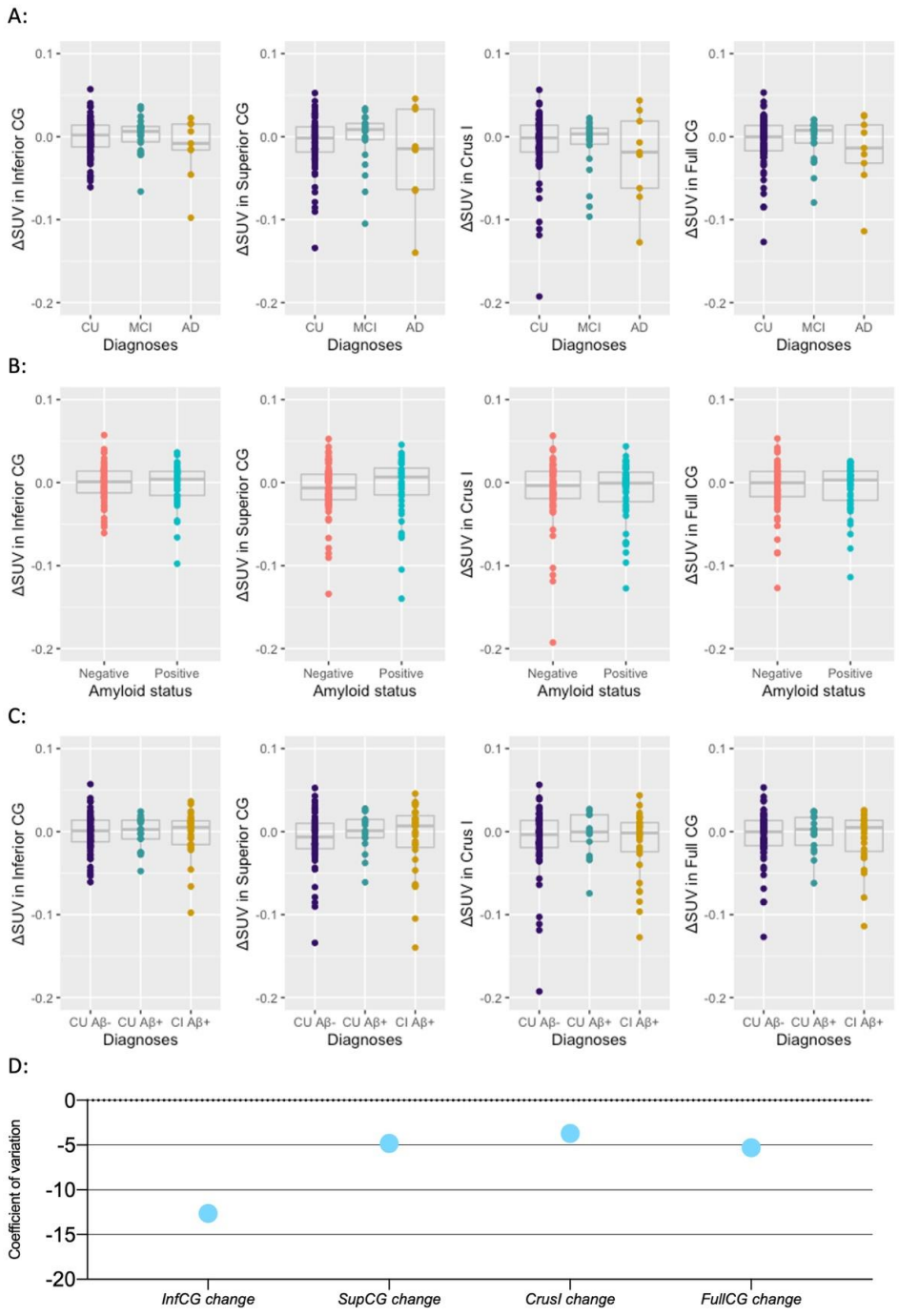

<u>Figure 1</u>: Annualized longitudinal changes in [^{18}F]MK6240 SUV in cerebellar candidate reference regions. ΔSUV of [^{18}F]MK6240 was not significantly different across A) diagnosis, B) Aβ status, C) diagnosis and Aβ status. D) Coefficient of variation of longitudinal changes in SUV within reference regions. Δ = change calculated as $\frac{(follow\text{-}up\ SUV\ -baseline\ SUV)}{time\ (years)}$.

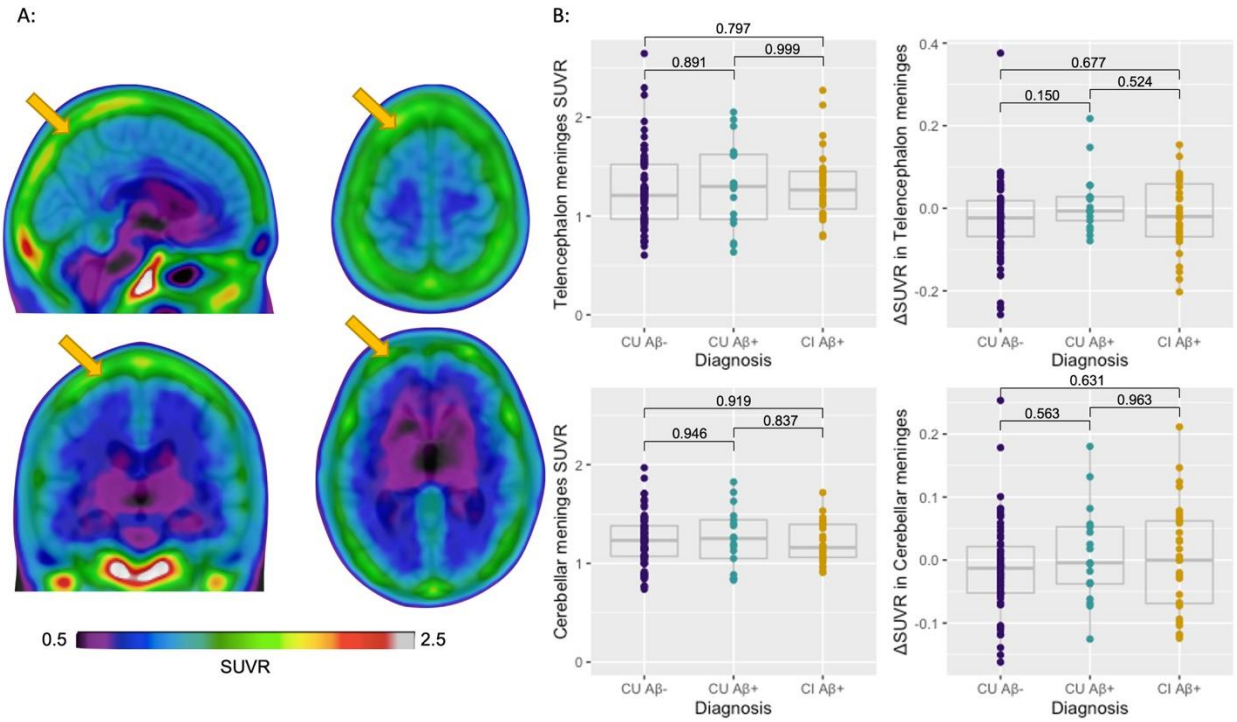

<u>Figure 2</u>: Cross-sectional and longitudinal meningeal [^{18}F]MK6240 SUVR across groups. A) Representative [^{18}F]MK6240 average SUVR image in cognitively unimpaired young individuals. B) Cross-sectional and longitudinal changes in [^{18}F]MK6240 (ΔSUVR) in the telencephalon and cerebellar meninges did not indicate significant differences depending on diagnosis and Aβ status. Δ = change calculated as $\frac{(follow\text{-}up\ SUVR - baseline\ SUVR)}{time\ (years)}$. Yellow arrows indicate the meninges.

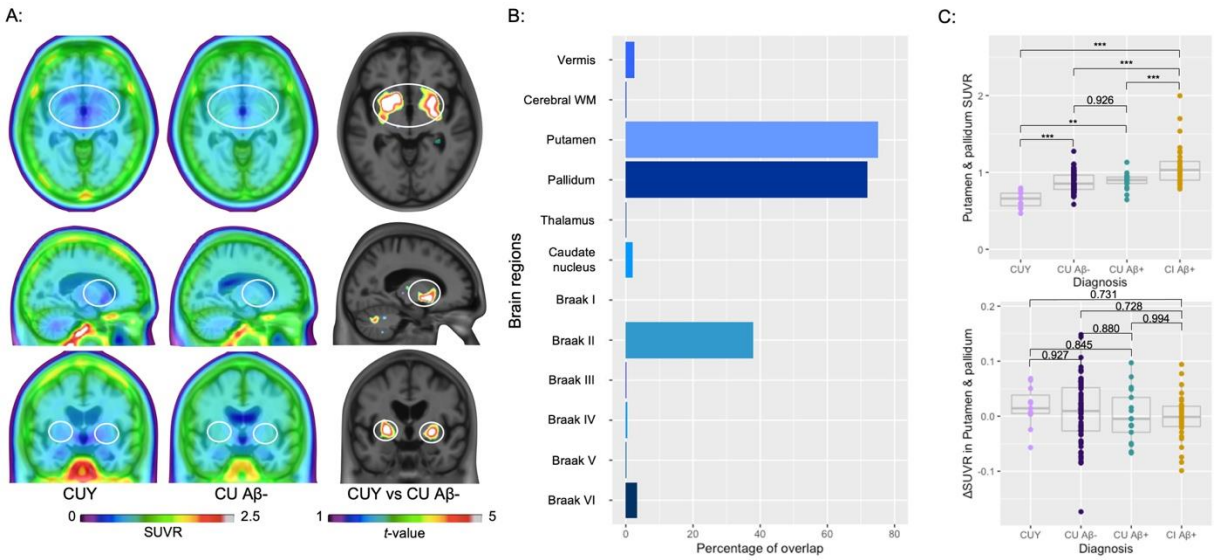

<u>Figure 3</u>: [^{18}F]MK6240 age-related retention. A) [^{18}F]MK6240 average SUVR image in cognitively unimpaired young (CUY) and cognitively unimpaired older adults (CU) Aβ negative individuals do not seem to show strong differences visually. T-test between the two groups depicts age-related retention in the putamen, the pallidum, cortical regions, and the cerebellar white matter. B) Percentage of overlap between age-related t-map and anatomical brain regions. C) Longitudinal changes (ΔSUVR) in [^{18}F]MK6240 SUVR values in the putamen/pallidum did not present significant differences across groups, whereas cross-section SUVR was higher in CI individuals, and lower in the CUY group. *P*-values portrayed as p<0.001=***, p<0.005=**. Δ = change calculated as $\frac{(follow\text{-}up\ SUVR - baseline\ SUVR)}{time\ (years)}$.

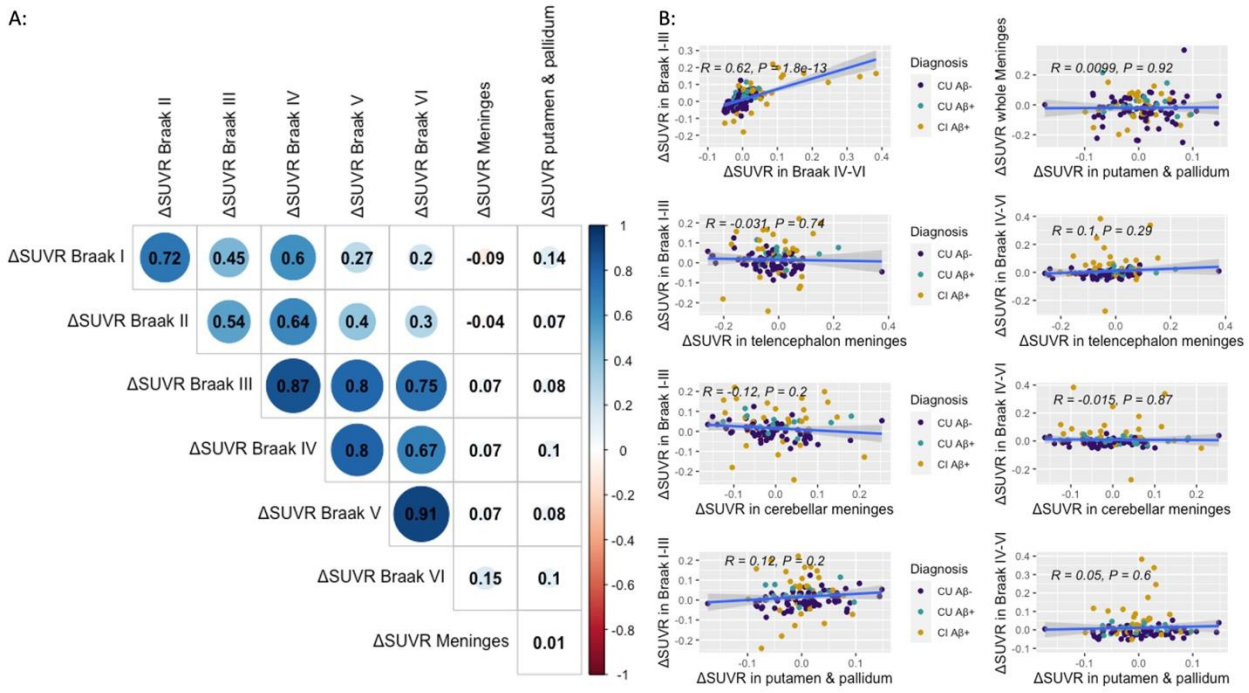

<u>Figure 4</u>: Correlations between longitudinal changes in SUVR in age-related, meningeal, and target regions. We assessed ΔSUVR values in regions presenting target (Braak I-VI), off-target (both telencephalon and cerebellar meninges), and age-related (putamen/pallidum) tracer uptake. We observed strong correlations between ΔSUVR among target regions; however, those did not correlate with ΔSUVRs in off-target and age-related regions. A) The matrix and B) plots present the estimates of Pearson correlations between regions. Δ = change calculated as $\frac{(follow\text{-}up\ SUVR - baseline\ SUVR)}{time\ (years)}$.

Tables:

Table 1: Demographics: Dataset used to assess age-related retention.

	CUY (N=37)	**CU Aβ- <65yo (N=27)**	**P-value**
Age (mean (SD))	23.41 (3.3)	58.09 (9.2)	<0.001
Sex (Female (%))	24 (64.9)	13 (48.1)	0.28
Years of education (mean (SD))	16.91 (2.5)	15.41 (3.4)	0.0167
MMSE (mean (SD))	29.86 (0.4)	29.22 (0.9)	<0.001
CDR (mean (SD))	0.00 (0.0)	0.00 (0.0)	NA

Table 2: Longitudinal dataset

	CUY	**CU Aβ-**	**CU Aβ+**	**CI Aβ+**	**P-value**
Age (mean (SD))	22.65 (1.9)	68.44 (9.8)	74.91 (5.1)	71.44 (5.3)	<0.001
Sex (Female (%))	8 (72.7)	41 (62.1)	14 (82.4)	14 (45.2)	0.0668
Years of education (mean (SD))	16.18 (1.7)	16.27 (4.1)	14.65 (2.4)	15.13 (3.4)	0.2
MMSE (mean (SD))	29.82 (0.6)	29.21 (1.1)	29.00 (1.0)	26.06 (4.6)	<0.001
CDR (mean (SD))	0.00 (0.0)	0.00 (0.0)	0.00 (0.0)	0.65 (0.4)	<0.001

Table 3: Coefficient of variation of cerebellar regions across diagnosis, at baseline, at follow-up and longitudinal changes.

	All	**CU Aβ-**	**CU Aβ+**	**CI Aβ+**
InfCG BL	0.19	0.18	0.14	0.22
SupCG BL	0.27	0.24	0.19	0.32
CrusI BL	0.25	0.26	0.19	0.28
FullCG BL	0.22	0.22	0.19	0.24
InfCG FU	0.17	0.18	0.16	0.17
SupCG FU	0.25	0.21	0.21	0.29
CrusI FU	0.22	0.21	0.22	0.25
FullCG FU	0.20	0.20	0.21	0.19
Δ*InfCG*	-12.64	-14.35	-11.12	-11.03
Δ*SupCG*	-4.83	-3.79	-52.03	-5.05
Δ*CrusI*	-3.71	-3.84	-7.48	-2.93
Δ*FullCG*	-5.30	-5.47	-9.63	-4.28

The longitudinal change was calculated using the formula: $\Delta=\frac{(follow-up\ SUV\ -baseline\ SUV)}{time\ (years)}$.

Table 4: *P*-values of the two-tailed t-test between baseline and follow-up SUV across cerebellar regions in individuals divided by diagnosis

	All	**CU Aβ-**	**CU Aβ+**	**CI Aβ+**
InfCG	0.67	0.81	0.72	0.83
SupCG	0.27	0.21	0.94	0.66
CrusI	0.09	0.18	0.72	0.31
FullCG	0.25	0.40	0.76	0.46

Supplementary material

Supplementary tables:

Supplementary Table 1: Mean and standard deviations of the injected dose and weight for each diagnostic group.

	CUY (N=31)	CU Aβ- (N=66)	CU Aβ+ (N=17)	CI Aβ+ (N=11)	P-value
Injected dose in MBq (mean (SD))	227.97 (27.9)	237.81 (24.8)	240.50 (27.8)	222.34 (29.0)	0.115
Weight in KG (mean (SD))	72.26 (14.6)	70.90 (13.7)	62.66 (10.6)	68.77 (15.8)	0.094

Supplementary Table 2: Size and images of the different reference regions assessed.

Cerebellum regions	*Inferior CG*	*Crus I*	*Superior CG*	*Full CG*
Size (voxels)	47194	35584	46394	129172
Image	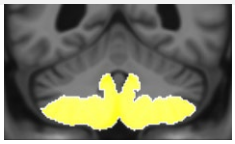	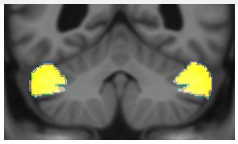	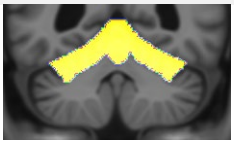	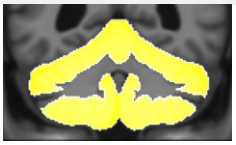

Supplementary Table 3: Sensitivity of scanner at baseline and follow-up based on diagnosis. We observed no significant differences among diagnostic group, at either baseline or follow-up visits.

A. Sensitivity as baseline scans

	CUY (N=11)	CU Aβ- (N=66)	CU Aβ+ (N=17)	CI Aβ+ (N=31)	P-value
Sensitivity, % (mean (SD))	6.65 (0.4)	6.54 (1.0)	6.54 (0.8)	6.54 (1.0)	0.807

B. Sensitivity as follow-up scans

	CUY (N=11)	CU Aβ- (N=66)	CU Aβ+ (N=17)	CI Aβ+ (N=31)	P-value
Sensitivity, % (mean (SD))	6.63 (0.3)	6.63 (0.3)	6.73 (0.1)	6.27 (0.3)	0.144

Supplementary Table 4: Mean and standard deviation of ΔSUV in different cerebellar reference regions.

	All diagnoses
ΔSUV InfCG (mean ± sd)	0.00 ± 0.02
ΔSUV SupCG (mean ± sd)	0.01 ± 0.03
ΔSUV CrusI (mean ± sd)	0.01 ± 0.04
ΔSUV FullCG (mean ± sd)	0.01 ± 0.03

Supplementary Table 5: *P*-values of the differences between baseline and follow-up assessments of different cerebellar regions across various diagnostic groups, including CUY.

	All	**CUY**	**CU Aβ-**	**CU Aβ+**	**CI Aβ+**
InfCG	0.441	0.397	0.812	0.720	0.830
SupCG	0.168	0.295	0.211	0.943	0.662
CrusI	0.045	0.321	0.178	0.722	0.310
FullCG	0.140	0.341	0.400	0.756	0.457

Supplementary Table 6: High and low meningeal retention. Individuals were categorized as high and low meningeal binders based on the median of the sample. A. Characteristics of the sample. B. T-test of ΔSUVR in Braak regions and meningeal retention status.

A: Diagnostic groups in high and low meningeal binders

	High (N=62)	**Low (N=63)**	**P-value**
Diagnosis			0.81
CUY, N(%)	6 (9.7%)	5 (7.9%)	
CU Aβ-, N (%)	32 (51.6%)	34 (54.0%)	
CU Aβ+, N (%)	10 (16.1%)	7 (11.1%)	
CI Aβ+, N (%)	14 (22.6%)	17 (27.0%)	

B: T-test of ΔSUVR in high and low meningeal binders

	High (N=62)	**Low (N=63)**	**P-value**
ΔSUVR in Braak I-III	0.02 (0.1)	0.01 (0.1)	0.453
ΔSUVR in Braak IV-VI	0.02 (0.1)	0.00 (0.1)	0.25

Supplementary Table 7: T-test between baseline and follow-up values in Braak IV-VI, in the CUY and CU Aβ- older adults, using different reference regions.

	***p*-value**
Braak IV-VI using InfCG	0.2970
Braak IV-VI using SupCG	0.8150
Braak IV-VI using CrusI	0.6825
Braak IV-VI using FullCG	0.4520

Supplementary figures:

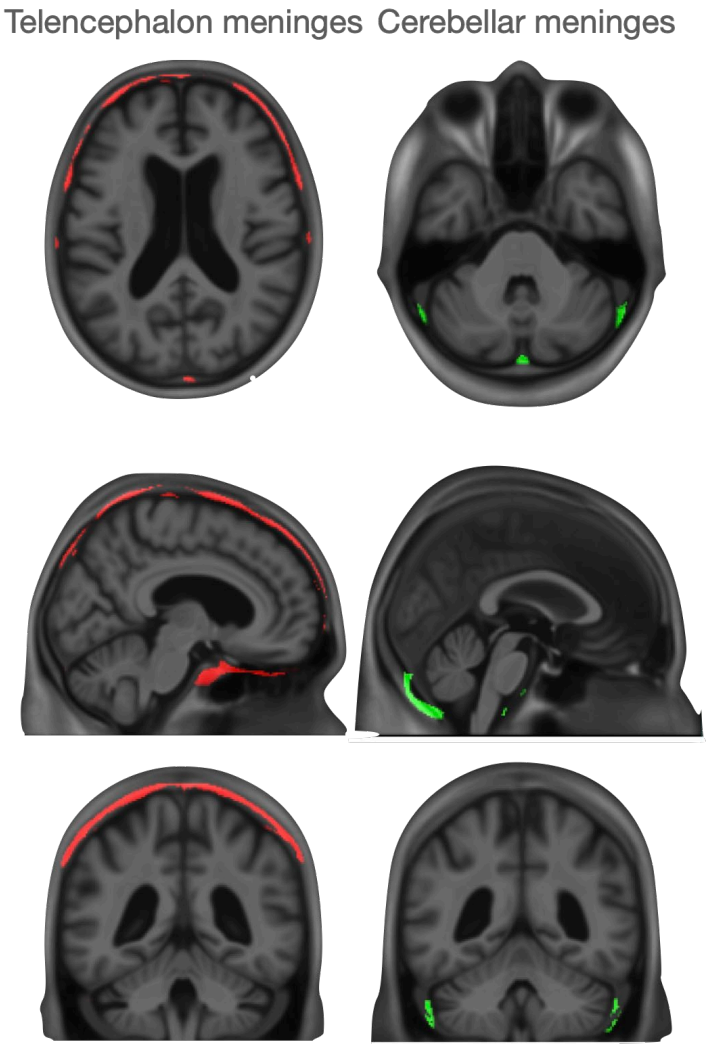

Supplementary Figure 1: Mask used to calculate telencephalon (red) and cerebellar (green) meningeal binding. This mask was defined as region having >85% probability to present high binding in CU individuals.

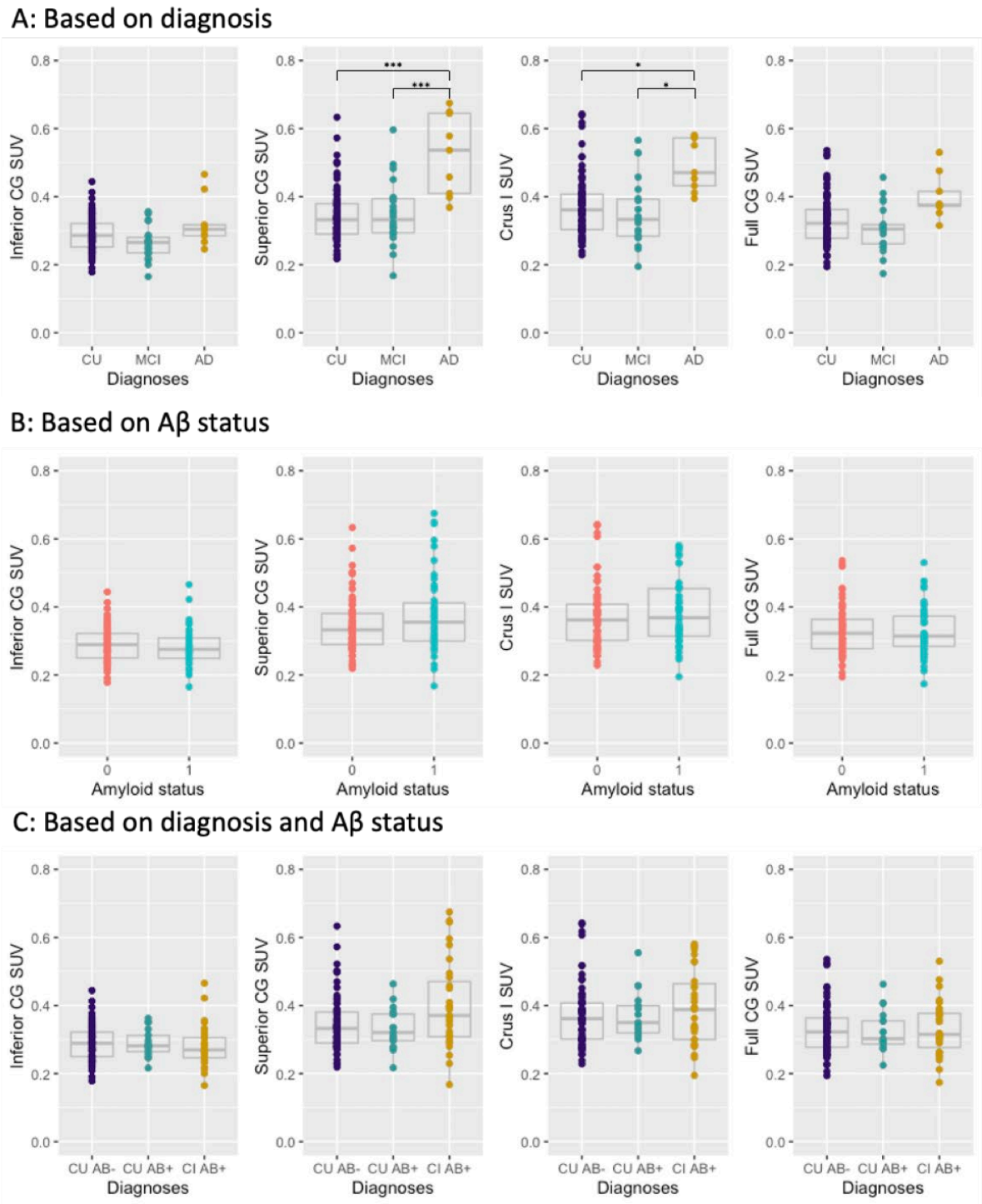

Supplementary Figure 2: Cross-sectional [^{18}F]MK6240 SUV in different cerebellar regions. Cross-sectional [^{18}F]MK6240 SUV values did not demonstrate significant differences based on A) diagnosis, B) amyloid-β status C) diagnosis and amyloid-β status. *P*-values portrayed as *p*-value < 0.001=***, *p*-value < 0.5=*.

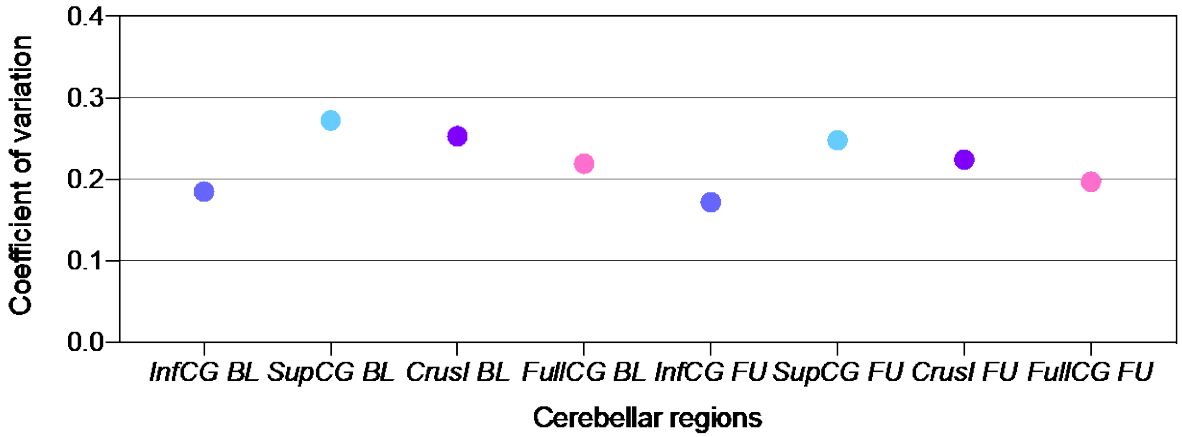

Supplementary Figure 3: Coefficient of variation of [^{18}F]MK6240 SUV in cerebellar regions, at baseline and follow-up visits.

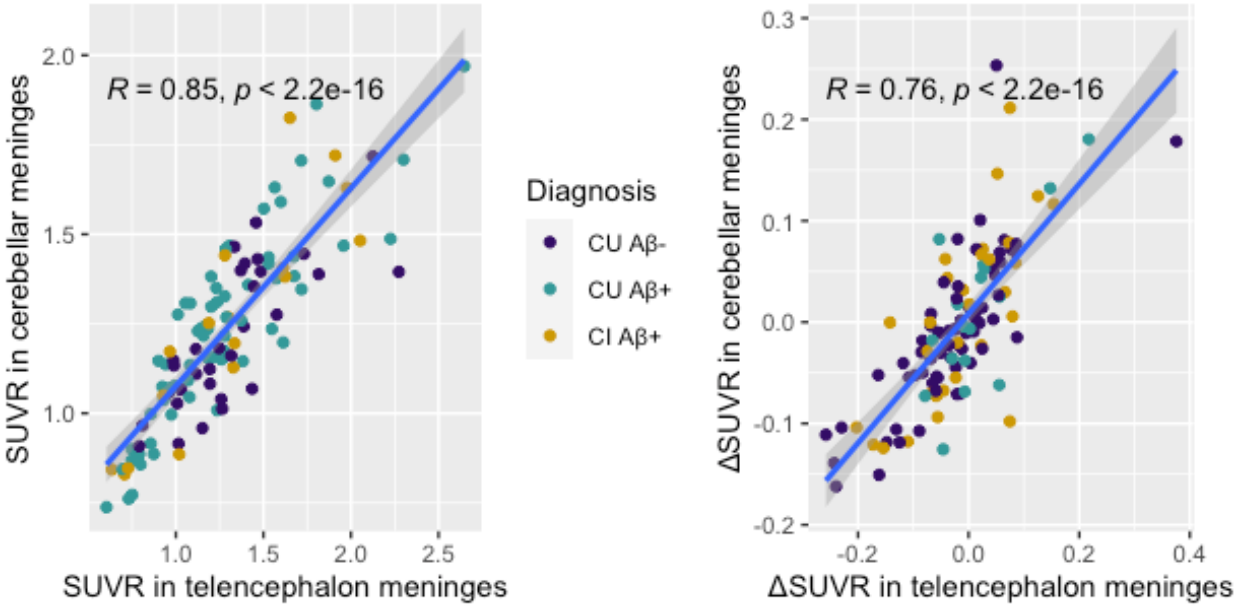

Supplementary Figure 4: Correlation between cross-sectional and longitudinal changes in telencephalon meninges SUVR and cerebellar meninges SUVR. Δ = change calculated as $\frac{(follow\text{-}up\ SUVR - baseline\ SUVR)}{time\ (years)}$. We observed a strong correlation between the two, cross-sectionally and longitudinally.

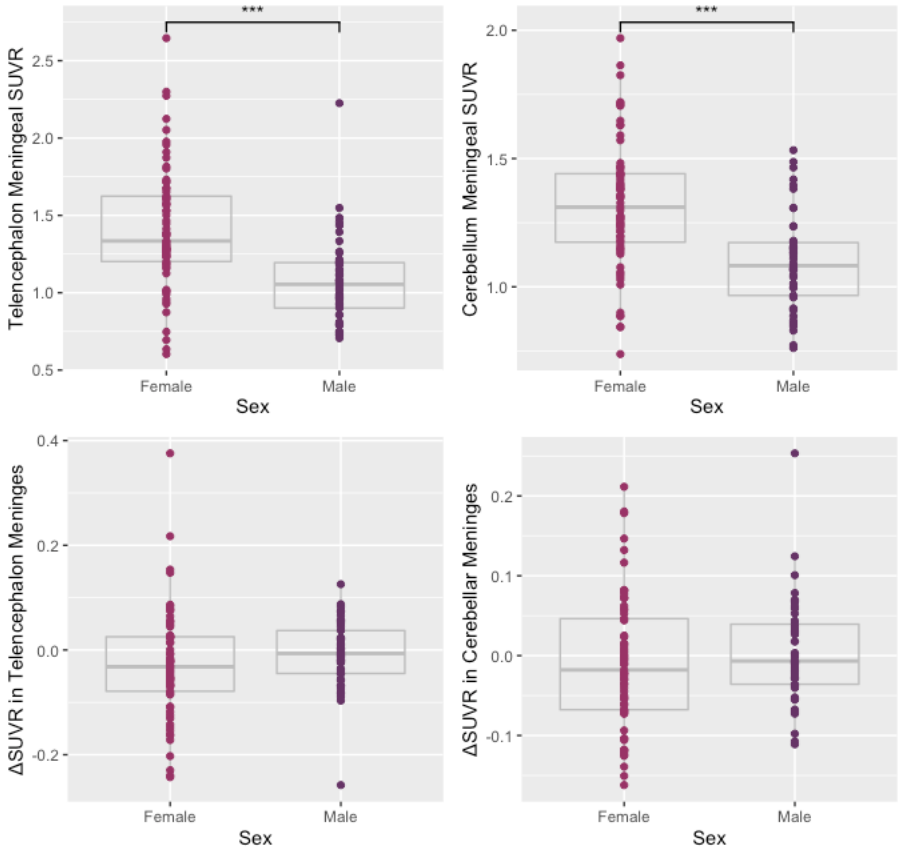

Supplementary Figure 5: Sex differences in meningeal retention. Females present higher meningeal SUVR in the telencephalon and cerebellar meninges, as compared to males cross-sectionally. However, there are no significant differences longitudinally. *P*-values portrayed as *p*-value < 0.001=***.

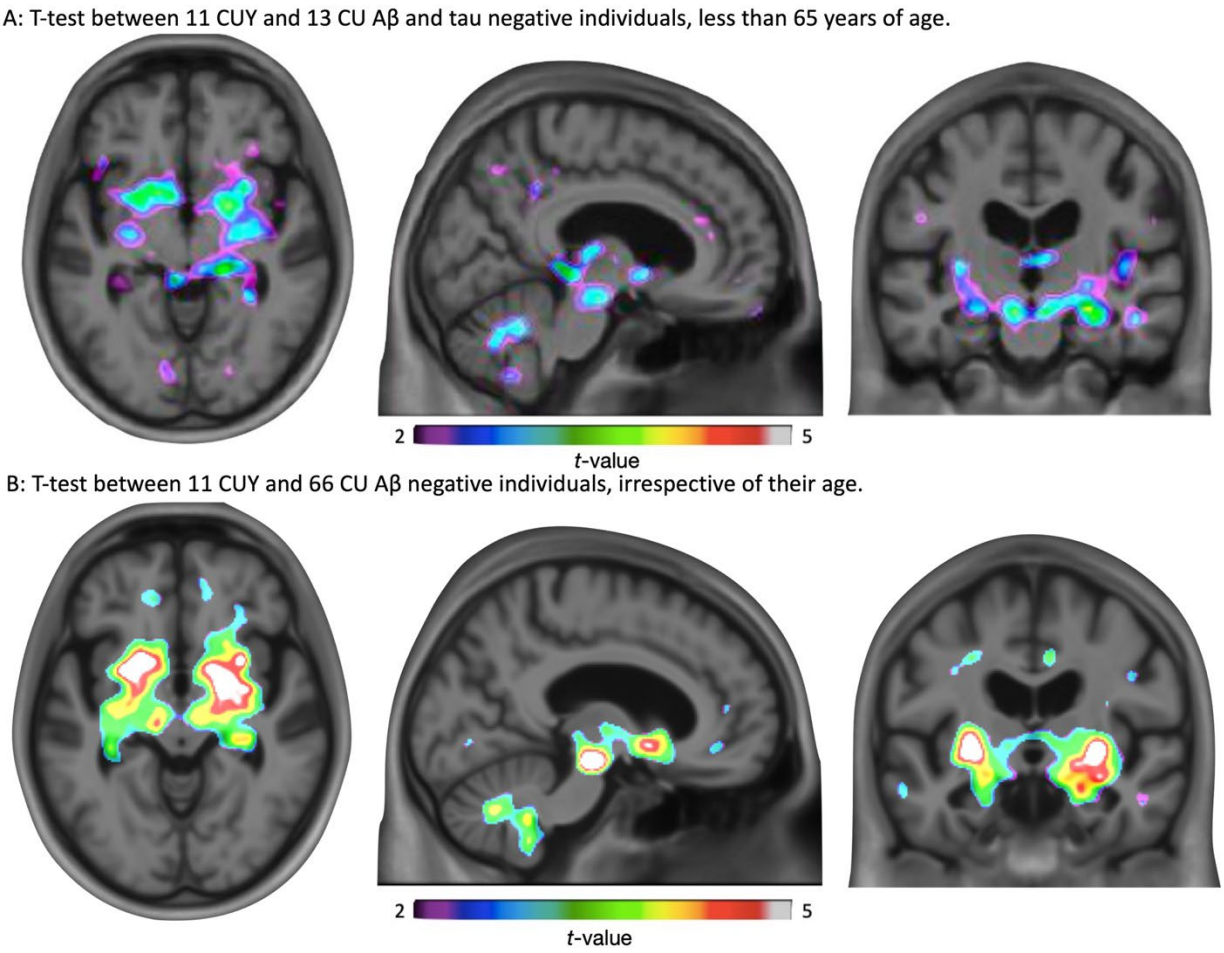

Supplementary Figure 6: Baseline t-test between cognitively unimpaired groups in the longitudinal sample. A. Between CUY (<35 years of age, N = 11) and CU Aβ and tau negative (<65 years of age, N = 13) included in the longitudinal sample. B. Between CUY (<35 years of age, N = 11) and 66 CU Aβ negative (irrespective of their age) included in the longitudinal sample.

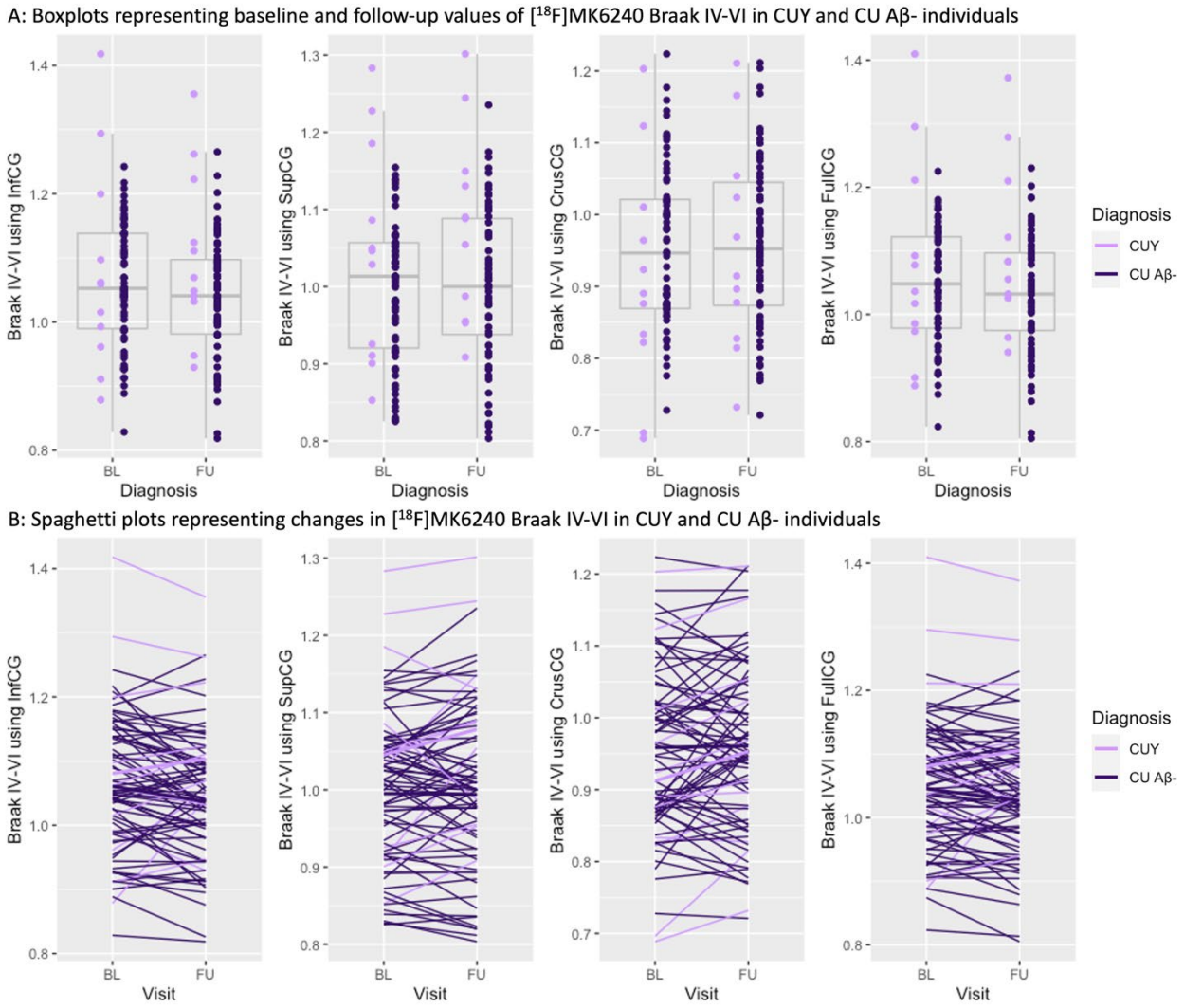

Supplementary Figure 7: Changes between baseline and follow-up values in Braak IV-VI, in CUY and CU Aβ- individuals. No significant changes were observed. A: Boxplots representing baseline and follow-up values. B. Spaghetti plots representing individuals changes between baseline and follow-up values.